Journal of Power and Energy Engineering, 2026, 14(3), 27-52
https://www.scirp.org/journal/jpee
ISSN Online: 2327-5901
ISSN Print: 2327-588X

Optimisation of Wireless Energy Transmission by Resonant Magnetic Coupling

Taguia Kana Borel[1], Tchoffo Houdji Etienne[2,3*], Nsouandele Jean Luc[1,2], Yeremou Tamtsia Aurélien[1]

[1]National Advanced School of Engineering of Douala, University of Douala, Douala, Cameroon
[2]National Advanced School of Engineering of Maroua, University of Maroua, Maroua, Cameroon
[3]Technology and Innovation Support Center/Advanced School of Mines Processing and Energy Resources, The University of Bertoua, Bertoua, Cameroon
Email: *tchoffohoudji@gmail.com

How to cite this paper: Taguia Kana, B., Tchoffo Houdji, E., Nsouandele, J.L. and Yeremou Tamtsia, A. (2026) Optimisation of Wireless Energy Transmission by Resonant Magnetic Coupling. *Journal of Power and Energy Engineering*, **14**, 27-52.
https://doi.org/10.4236/jpee.2026.143002

Received: January 25, 2026
Accepted: March 16, 2026
Published: March 19, 2026

Abstract

Since the end of the 20th century, portable electronic devices (computers, telephones, etc.) have become increasingly present in our daily lives. Although popular, these electronic devices are highly dependent on the short operating time of their power supply (batteries). For the user, the convenience of portable electronics is gradually being compromised by the need to recharge the batteries almost all the time. For devices that cannot be connected to a charger, the problem of battery replacement becomes even more delicate. To provide a solution to this problem, this article proposes a wireless power transfer system using inductive coupling. It uses the resonance phenomenon to optimize the system efficiency and the power transferred to the load. Using Visual Studio Code software, which is a cross-platform code editor developed by Microsoft, based on the Electron framework and primarily written in TypeScript, an enhanced version of JavaScript, five cases have been proposed and simulated according to the characteristics of the passive components of the system, namely inductance, capacitance and resistance. These are the following configurations: 1) non-resonant circuit, 2) circuit with series resonance in the primary, 3) circuit with series resonance in the secondary, 4) circuit with series-series resonance in the primary and secondary, and 5) circuit with parallel resonance in the primary and series resonance in the secondary. This last configuration is a new, improved configuration proposed. The results obtained show that the power transferred to the load (2034 W) by the proposed improved configuration, is 1.04 times higher than that transferred by the circuit with series resonance in the primary and secondary (1940 W), and 3228 times higher than that transferred by the non-resonant circuit (0.63 W). The efficiency of the proposed improved configuration is 70%. It is 3 times higher than that of the

non-resonant circuit (22%). These results also show that with a judicious choice of inductance, capacitance values and frequency, it is possible to obtain a theoretical efficiency of 99.981% and a theoretical power transferred to the load of 7027.97 W.

Keywords

Mobile Electrical System, Energy, Wireless Transmission, Resonant Circuit, Optimization

1. Introduction

Energy is an important factor in country's development. It is also a tool for social stability. It plays a fundamental role in reducing extreme poverty and hunger and in ensuring basic education for all in both urban and rural areas. Cameroon, like most countries in sub-Saharan Africa, faces a serious problem of access to electricity. According to a report published on 11 August 2017 by the Cameroonian Agency for Rural Electrification (ARE), 2960 out of 13,634 localities are electrified, a rate of 21.7% [1]. This situation is mainly due to two factors: insufficient energy supply and losses due to the joule effect on the transmission and distribution networks. In addition, recent years have seen the massive development of a wide range of portable electronic devices, both in the consumer sector, such as smartphones or tablets, and in industrial applications, such as wireless sensor networks or medical applications. A study carried out shows that by 2023, 70% of the world's population will own a smartphone in 2023, or five billion six hundred million people [2]. The general trend is to move more and more towards miniaturization of devices in order to facilitate their portability and integration into everyday life. One of the most sensitive issues to be addressed is the power source for these devices. In most cases, the use of power cables is not an option, due to the "nomadic" nature of these devices. The majority of today's portable devices use batteries as their power source. In the case of compact devices, batteries tend to take up most of the available volume, making further miniaturization almost impossible, while adding mass and increasing cost [3]. The autonomy of such devices is limited by the trade-off between the amount of available power and size. Batteries need to be replaced or recharged regularly. This almost constant recharging, which must be carried out several times a day, is bulky, heavy and disruptive to our working hours. In addition, the fact that these recharges are wired means that these electronic devices are increasingly losing their portable character and require us to be in the presence of an electrical outlet or power source throughout the day.

Even more worrying is the environmental impact of all these batteries in the world, because when they decompose, they release greenhouse gases into the atmosphere, contributing to global warming. According to the Swedish Agency for Research and the Environment, each kWh of batteries produced generates the

equivalent of 150 to 200 kg of CO_2 [4]. It is important to emphasize that in some areas of applications, batteries simply cannot be used because of their size (biomedical micro-implants) or their inaccessibility (strain sensors implanted in concrete structures for 40 years), and these cannot be continuously powered by an electric wire because of their location and use. Nevertheless, given their importance, it is necessary to power these devices.

One solution to the various problems mentioned above is wireless energy transfer. This process allows energy to be transferred from one point to another without the need to connect them with an electrical cable [3]. Non-contact energy transfer is now a proven technology with undeniable advantages in terms of safety (no direct electrical contact) and ergonomics [3] [5]. Magnetic induction energy transfer has many applications, ranging from mobile electronics (charging of smartphones, laptops, GPS, etc.), to transport (cars, buses, trams, etc.), including active medical implants (pacemakers, defibrillators, hearing aids, insulin pumps, brain valves, etc.) [3] [6]-[8]. Several authors have worked on wireless power transmission. One of the pioneers of wireless transmission was Nicola Tesla in 1896. He worked on long-distance power transmission by transmitting a radiofrequency signal over a distance of almost 50 km in 1896 [9] [10]. In 1899, he also succeeded in transmitting a very high voltage to power 200 light bulbs and an electric motor more than 40 km away. However, the electric arcs generated by the use of very high voltages made the application dangerous for nearby users [9] [10]. In the 1960s, William C. Brown began experimenting with wireless energy transfer (WET) using microwave tubes such as magnetrons and klystrons [11]. Then in 1963, he developed a rectifier antenna to receive electromagnetic waves and convert them into DC voltage, with an output power of 4 W and 7 W, with efficiencies of 50% and 40% respectively [11]. Also in 1964, he performed a demonstration on a 2.3 kg electric helicopter model powered by a microwave beam from the ground. It flew for 10 hours at an altitude of 18 m [11]. This demonstrated the usefulness of microwave energy transfer and launched several research campaigns to transmit high power over long distances. Concepts were even developed for powering satellites in orbit around the Earth, using very high power with directional beams [12]. Based on the work of Nicola Tesla and William C. Brown, NASA successfully tested 34 kW over a distance of 1.55 km using microwaves at 2.45 GHz with an efficiency of 54% in 1975 [11]. In 2006, Soljacic and the MIT (Massachusetts Institute of Technology) research laboratory were able to light a 60 W bulb at 2 m, with an efficiency of 40% [13] [14]. In 2014, Ahafhaf Amine *et al.*, propose a wireless charging scheme for mobile phones, but the efficiency does not exceed 40% [15]. In the same year, Wang Wei worked on wire power transmission (WPT) based on magnetic coupled resonance, where the transmission distance could reach more than 2 or 3 times the dimension of the transmitter [16]. However, when the coupling factor is low, a large part of the energy is lost [16]. In 2017, Boudjema notes that the voltage and power strongly depend on the electrical characteristics (frequency, compensation capacity) and the geometrical characteristics

of the coils (coil dimension, relative distance of the coils) [17]. In 2018, Zhang *et al.,* proposed an improved 3-coil wireless power link to increase the spacing distance and power of the system. The results of their work show that the transmission power can reach 120 W at a distance of 2.5 m [18]. In 2020, Yan *et al.*, worked on a wireless energy transmission system based on a coil structure, with the aim of powering a drone. The results of their studies show that they were able to transmit a power of 65.77 W and achieved a system efficiency of 62.44% [19]. In 2022, Taoutaou *et al.,* studied and simulated a resonant energy transfer system, where they managed to track the frequency, which allows to have the resonant frequency which in turn controls the active power produced [20]. This resonant frequency helps to maintain the power at its maximum point in order to have an optimal energy transfer. In 2023, Tag worked on pulse waveform optimization for wireless energy transfer, where he managed to optimize the output capacitor by setting the RC constant of the circuit [21]. In the same year of 2023, Yadav and Bera worked on the effect of ferrite shielding and its thickness, enabling optimization of wireless energy transmission. In their study, they achieved an efficiency of 98.88% to 99.7360% at a frequency of 6.78 MHz for a rectangular ferrite coupler 5 mm to 50 mm thick [22]. In 2024, Nebrida demonstrated the importance of coupled resonance in a wireless transmission circuit. In his study, he showed that at the resonance frequency, the system is optimized [23].

From the various studies carried out on wireless energy transmission, two conclusions can be drawn:

- Far-field energy transmission technology has a high health impact according to the ICNIRP (International Commission on Non-Ionizing Radiation Protection) standard, which specifies the average SAR (Specific Absorption Dose) values that can be tolerated by the human body depending on the operating frequency. According to this standard, for a frequency in the range 100 kHz - 10 GHz, the average SAR over the whole body for the public is 0.5 W/kg [24] [25].
- Near-field power transmission technology, which has no impact on health, has an efficiency not exceeding 50% and the power available at the secondary load is low [26]-[29].

Based on these findings, and considering that the far-field power transmission technology is dangerous to nearby users, the research work focuses on the near-field power transmission technology.

2. Methods/Experimental

Knowing that in the previous specific case of technology, studies have shown that the efficiency does not exceed 50%, the aim of the present work focuses on optimizing the efficiency and the power transmitted to the load using the resonance phenomenon. To achieve this goal, a coupled resonance is created between the transmitter and the receiver in order to transmit the maximum power and minimize losses. Different cases are studied: 1) circuit without resonance, 2) circuit

with series with resonance in the primary, 3) circuit with series resonance in the secondary, 4) circuit with series-series resonance in the primary and secondary, and 5) circuit with parallel resonance in the primary and series resonance in the secondary; a new improved configuration is proposed. The rest of the work is structured around the principle of wireless energy transmission (Section II.1); the modelling of the wireless energy transmission system (Section II.2); the modeling of the different cases of the wireless energy transfer system (WETS) by inductive coupling (Section II.3); the results and discussion (Section III) and a conclusion (Section VI) will summarize the main results of the work developed. To simulate each of the presented scenarios, we will use Visual Studio Code, a cross-platform code editor developed by Microsoft, based on the Electron framework and primarily written in TypeScript, an enhanced version of JavaScript. Two libraries will be used: "numpy as np" and "matplotlib.pyplot as plt", which respectively represent the basic library for numerical computation and the standard library for data visualization. The first allows manipulation of multidimensional data arrays, and the second allows the generation of high-quality graphs (curves, histograms, scatter plots, 3D graphs).

2.1. Diagram of the Principle of the Wireless Energy Transmission

Wireless power transmission consists of a transmitter part powered by an AC power source and a receiver part connected to a load, as shown in **Figure 1**.

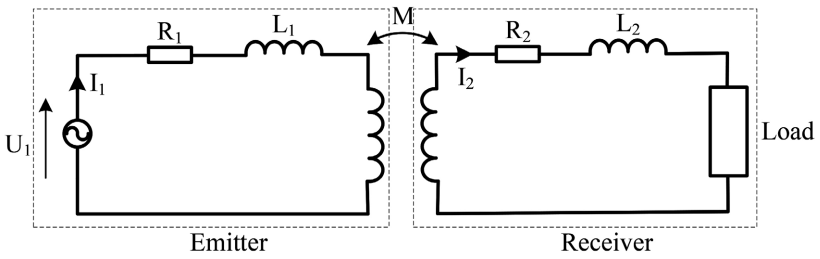

Figure 1. Schematic representation of the principle of the wireless energy transmission [17].

The principle of wireless energy transfer by inductive magnetic coupling is based on the electromagnetic induction phenomenon. When an alternating current powers the transmitter coil, a magnetic field is created, and since the current is alternating, the magnetic field created is variable. The receiver coil, immersed in this variable magnetic field, generates an electromotive force (EMF) at the terminal of the receiver coil in accordance with the Lenz-Faraday law. Therefore, this EMF is used at the secondary level to power loads (telephones, computers, televisions, light bulbs, etc.) [30].

2.2. Mathematical Model of the Wireless Energy Transmission System

The coupling relationship between the currents of the different windings " p and q " is given by Equation (1) [17] [31].

$$\frac{2\pi}{\sigma}\frac{r(p)}{s(p)}I(p)+j\omega\mu_0 r(p)\sum_{q=1}^{N}G(p,q)I(q)=u(p) \quad (1)$$

With

- $I(p)$ and $u(p)$ are respectively the elementary current and voltage of the "p" winding.
- $r(p)$ and $s(p)$ are respectively the radius and the surface of the receiving point
- σ: Electrical conductivity
- μ_0: Magnetic permeability of vacuum
- ω: the electrical pulsation
- $G(p,q)$: Electric induction

Applying Equation (1) to the two coils gives Equation (2):

$$\begin{cases}\left(\sum_{p=1}^{N_1}\frac{2\pi}{\sigma s}r_1(p)+j\omega\mu_0\sum_{p=1}^{N_1}r_1(p)\sum_{q=1}^{N_1}G_1(p,q)\right)I_1+j\omega\mu_0\sum_{p=1}^{N_1}r_1(p)\sum_{q=1}^{N_2}G_{12}(p,q)=U_1\\ \left(\sum_{p=1}^{N_2}\frac{2\pi}{\sigma s}r_2(p)+j\omega\mu_0\sum_{p=1}^{N_2}r_2(p)\sum_{q=1}^{N_2}G_2(p,q)\right)I_2+j\omega\mu_0\sum_{p=1}^{N_2}r_2(p)\sum_{q=1}^{N_1}G_{21}(p,q)=U_2\end{cases} \quad (2)$$

Therefore, the system equation is:

$$\begin{cases}(R_1+jL_1\omega)I_1+jM\omega I_2=U_1\\ jM\omega I_1+(R_2+jL_2\omega)I_{22}=U_2\end{cases} \quad (3)$$

With:

- N: Number of coils; $\omega=2\pi f$: Electrical pulsation; f: Frequency;
- R_1, R_2: Internal resistance of the coils; L_1, L_2: Self-inductance of the coils;
- M: Mutual inductance between the coils.
- U_1 and U_2: the primary and secondary voltages, respectively.

➢ Coil 1 parameters [17] [31]:

$$\begin{cases}R_1=\sum_{p=1}^{N_1}\frac{2\pi}{\sigma s}r_1(p)\\ L_1=\mu_0\sum_{p=1}^{N_1}r_1(p)\sum_{q=1}^{N_1}G_1(p,q)\end{cases} \quad (4)$$

➢ Coil 2 parameters [17] [27]:

$$\begin{cases}R_2=\sum_{p=1}^{N_2}\frac{2\pi}{\sigma s}r_2(p)\\ L_1=\mu_0\sum_{p=1}^{N_2}r_2(p)\sum_{q=1}^{N_2}G_2(p,q)\end{cases} \quad (5)$$

➢ The mutual between coils 1 and 2 is given by Equation (6) [17] [31]:

$$\begin{aligned}M=M_{12}=M_{21}&=\omega\mu_0\sum_{p=1}^{N_1}r_1(p)\sum_{q=1}^{N_2}G_{12}(p,q)\\ &=\omega\mu_0\sum_{p=1}^{N_2}r_2(p)\sum_{q=1}^{N_1}G_{21}(p,q)\end{aligned} \quad (6)$$

When the system output is connected to a resistive load, the output voltage is by Equation (7) [17] [27]:

$$\begin{cases}(R_1+jL_1\omega)I_1+jM\omega I_2=U_1 & (a)\\ jM\omega I_1+(R+R_2+jL_2\omega)I_2=0 & (b)\\ U_2=-RI_2 & (c)\end{cases} \quad (7)$$

Then

$$U_2 = \frac{-jMR\omega}{M^2\omega^2 + (R_1 + jL_1\omega) + (R + R_2 + jL_2\omega)} U_1 \tag{8}$$

2.3. Modeling of Wireless Energy Transfer System (WETS) by Inductive Coupling

The following basic parameters are used in the remainder of this paper:

- The mutual inductance M (which we will assume to be positive) is written:

$$M = K\sqrt{L_1 L_2} \tag{9}$$

With: K : the coupling coefficient; L_1 and L_2 : the inductance of the transmitter and receiver

Throughout the modelling, as the aim is to optimize wireless transmission when the primary and secondary coils are as far apart as possible, a very low coupling coefficient is used. Let $K = 0.1$. The mutual inductance is used in the equations for the transmitter and receiver circuits in the various wireless energy transfer schemes.

In the following, the coils used in the simulation have the following characteristics: Length $L = 45$ m , and section $S = 1.5$ mm^2 .

2.3.1. WETS with Non-Resonant Magnetic Coupling

The coil is modelled by the series connection of a self-inductance and a resistance, which is assumed to be independent of the frequency. The electrical circuit of this energy transfer system is shown in Figure 2.

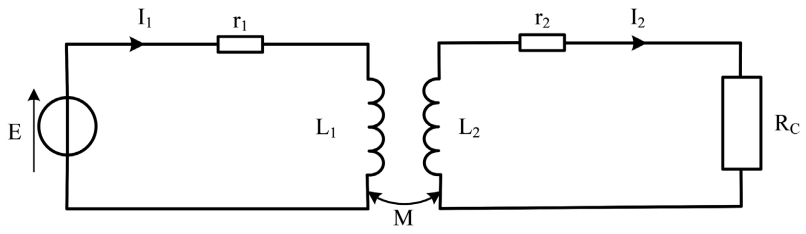

Figure 2. Electrical diagram of inductive coupling with a real coil, without resonance.

Let I_1 and I_2 be the complex amplitudes of the current intensities in the two circuits. In sinusoidal regime of pulsation ω , the mathematical model of the wireless energy transfer system (WETS) with non-resonant magnetic coupling for the transmitter and receiver circuits are given by Equations (10) and (11).

$$E = (jL_1\omega + r_1) I_1 + jM\omega I_2 \tag{10}$$

$$0 = (jL_2\omega + r_2 + R_C) I_2 + jM\omega I_1 \tag{11}$$

The following parameters can be derived from these equations:

- Current at the transmitter

$$I_1 = \frac{E(jL_2\omega + r_2 + R_C)}{(jL_1\omega + r_1)(jL_2\omega + r_2 + R_C) + (M\omega)^2} \tag{12}$$

- Current at the receiver

$$I_2 = \frac{jM\omega E}{\left(jL_1\omega + r_1\right)\left(jL_2\omega + r_2 + R_C\right) + \left(M\omega\right)^2} \tag{13}$$

- The power provided by the transmitter

$$P_1 = \frac{1}{2}Re\left(E \cdot I_1\right) = \frac{1}{2}Re\left(\left(jL_1\omega + r_1\right)I_1 + jM\omega I_2\right)I_1 \tag{14}$$

- The average power transmitted to the load resistance

$$P_2 = \frac{1}{2}R_C\left|I_2\right|^2 \tag{15}$$

2.3.2. WETS with Magnetic Coupling with Resonance in the Secondary

The electrical circuit for this wireless power transmission mode has a capacitor connected in series with the load as shown in **Figure 3**.

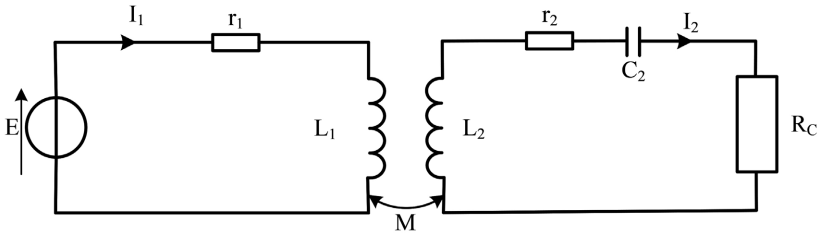

Figure 3. Electrical diagram of inductive coupling with resonance in the secondary.

The mathematical model describing the operation of the circuit of the wireless energy transfer system (WETS) with inductive coupling and resonance at the secondary is given by Equations (16) and (17).

$$E = \left(jL_1\omega + r_1\right)I_1 + jM\omega I_2 \tag{16}$$

$$0 = \left(\frac{1}{jC_2\omega} + jL_2\omega + r_2 + R_C\right)I_2 + jM\omega I_1 \tag{17}$$

From Equations (16) and (17), the following parameters can be derived:

- Current at the transmitter

$$I_1 = \frac{E\left(jL_2\omega + r_2 + R_C + \dfrac{1}{jC_2\omega}\right)}{\left(jL_1\omega + r_1\right)\left(jL_2\omega + r_2 + R_C + \dfrac{1}{jC_2\omega}\right) + \left(M\omega\right)^2} \tag{18}$$

- Current at the receiver

$$I_2 = \frac{jM\omega E}{\left(jL_1\omega + r_1\right)\left(jL_2\omega + r_2 + R_C + \dfrac{1}{jC_2\omega}\right) + \left(M\omega\right)^2} \tag{19}$$

The power provided by the transmitter

$$P_1 = \frac{1}{2}Re\left(E \cdot I_1\right) = \frac{1}{2}Re\left(\left(jL_1\omega + r_1\right)I_1 + jM\omega I_2\right)I_1 \tag{20}$$

The average power transmitted to the load resistance

$$P_2 = \frac{1}{2} R_C \left| I_{\underline{2}} \right|^2 \tag{21}$$

2.3.3. WETS with Magnetic Coupling with Resonance in the Primary

As shown in Figure 4, in this wireless power transfer mode, a capacitor is connected in series with the power source in the system circuit.

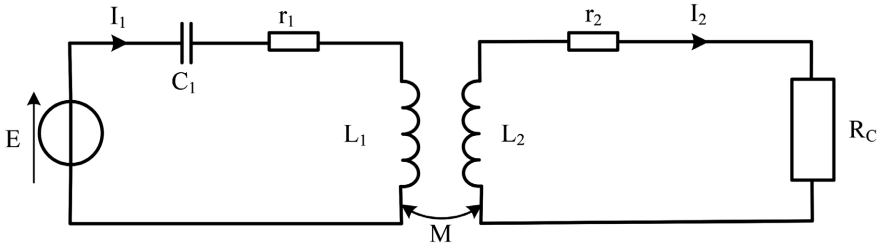

Figure 4. Electrical diagram of inductive coupling with resonance in the primary.

The mathematical model of this circuit is given by Equations (22) and (23).

$$E = \left(\frac{1}{jC_1 w} + jL_1\omega + r_1 \right) I_{\underline{1}} + jM\omega I_{\underline{2}} \tag{22}$$

$$0 = \left(jL_2\omega + r_2 + R_C \right) I_{\underline{2}} + jM\omega I_{\underline{1}} \tag{23}$$

- From these Equations (22) and (23), the following parameters can be derived Current at the transmitter

$$I_{\underline{1}} = \frac{E\left(jL_2\omega + r_2 + R_C \right)}{\left(jL_1\omega + r_1 + \frac{1}{jC_1\omega} \right)\left(jL_2\omega + r_2 + R_C \right) + \left(M\omega \right)^2} \tag{24}$$

- Current at the receiver

$$I_{\underline{2}} = \frac{jM\omega E}{\left(jL_1 w\omega + r_1 + \frac{1}{jC_1\omega} \right)\left(jL_2\omega + r_2 + R_C \right) + \left(M\omega \right)^2} \tag{25}$$

- The power provided by the transmitter

$$P_1 = \frac{1}{2} Re\left(E \cdot I_{\underline{1}} \right) = \frac{1}{2} Re\left(\left(jL_1\omega + r_1 + \frac{1}{jC_1\omega} \right) I_{\underline{1}} + jM\omega I_{\underline{2}} \right) I_{\underline{1}} \tag{26}$$

- The average power transmitted to the load resistance

$$P_2 = \frac{1}{2} R_C \left| I_{\underline{2}} \right|^2 \tag{27}$$

2.3.4. WETS with Magnetic Coupling with Resonance in the Primary and in the Secondary

In the electrical circuit of this wireless energy transfer mode system, one capacitor is connected in series with the power source and the other in series with the load as shown in Figure 5.

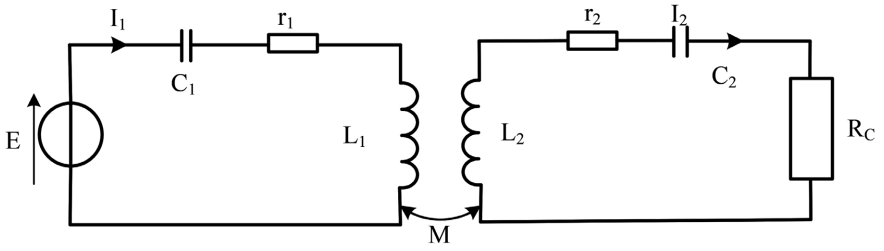

Figure 5. Electrical diagram of inductive coupling with resonance in the primary and in the secondary.

The mathematical model of this circuit is given by Equations (28) and (29).

$$E = \left(\frac{1}{jC_1 w} + jL_1\omega + r_1 \right) I_{\underline{1}} + jM\omega I_{\underline{2}} \tag{28}$$

$$0 = \left(jL_2\omega + r_2 + \frac{1}{jC_2\omega} + R_C \right) I_{\underline{2}} + jM\omega I_{\underline{1}} \tag{29}$$

From these equations, the following parameters can be derived:

- Current at the transmitter

$$I_{\underline{1}} = \frac{E\left(jL_2\omega + r_2 + \frac{1}{jC_2\omega} + R_C \right)}{\left(jL_1\omega + r_1 + \frac{1}{jC_1\omega} \right)\left(jL_2\omega + r_2 + \frac{1}{jC_2\omega} + R_C \right) + (M\omega)^2} \tag{30}$$

- Current at the receiver

$$I_{\underline{2}} = \frac{jM\omega E}{\left(jL_1\omega + r_1 + \frac{1}{jC_1\omega} \right)\left(jL_2\omega + r_2 + \frac{1}{jC_2\omega} + R_C \right) + (M\omega)^2} \tag{31}$$

- The power supplied by the transmitter

$$P_1 = \frac{1}{2} Re\left(E \cdot I_{\underline{1}} \right) = \frac{1}{2} Re\left(\left(jL_1\omega + r_1 + \frac{1}{jC_1\omega} \right) I_{\underline{1}} + jM\omega I_{\underline{2}} \right) I_{\underline{1}} \tag{32}$$

- The average power transmitted to the load resistance

$$P_2 = \frac{1}{2} R_C \left| I_{\underline{2}} \right|^2 \tag{33}$$

2.3.5. WETS with Parallel Resonance in the Primary and Series Resonance in the Secondary

In order to increase the power transferred to the load, a new configuration has been proposed in which a parallel LC circuit is connected to the source via a self-inductance coil with a low internal resistance has been proposed. This configuration arises from the fact that a parallel LC circuit to the primary would allow a much larger current in the coil (this being the sum of the current from the capacitor in parallel and from the source). The diagram of the proposed circuit is given in **Figure 6**. In the primary circuit, the capacitor is connected in parallel with the coil. This creates a parallel LC resonant circuit connected to the source via a self-

inductance coil L_0. The aim of this configuration is to obtain, at resonance, a current I_1 in the primary coil that is much larger than the current I_0 supplied by the source, with most of the current being provided by the capacitor. This configuration in the primary should make it possible to increase the power transmitted to the load. On the secondary, a capacitor is placed in series with the load in order to have a resonance that increases the efficiency of the circuit.

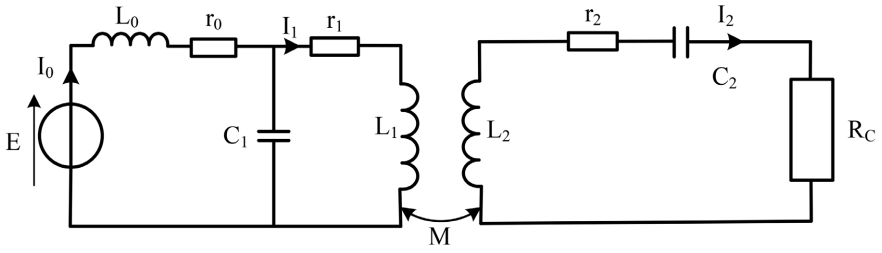

Figure 6. WETS optimization by resonance enhancement.

The mathematical model of this proposed new circuit is given by Equations (34) to (37).

$$E = \left(\frac{1}{jC_1\omega} + jL_0\omega + r_0\right)I_0 + \left(\frac{-1}{jC_1\omega}\right)I_1 + (0)I_2 \tag{34}$$

$$E = \left(jL_0\omega + r_0\right)I_0 + \left(jL_1\omega + r_1\right)I_1 + \left(jM\omega\right)I_2 \tag{35}$$

$$0 = (0)I_0 + \left(jM\omega\right)I_1 + \left(r_2 + R_C + \frac{1}{jC_2\omega} + jL_2\omega\right)I_2 \tag{36}$$

These equations can be put in the form of a matrix as in Equation (18)

$$\begin{pmatrix} jL_0\omega + r_0 + \dfrac{1}{jC_1\omega} & \dfrac{-1}{jC_2\omega} & 0 \\ jL_0\omega + r_0 & jL_1\omega + r_1 & jM\omega \\ 0 & jM\omega & jL_2\omega + r_2 + R_C + \dfrac{1}{jC_2\omega} \end{pmatrix} \begin{pmatrix} I_0 \\ I_1 \\ I_2 \end{pmatrix} = \begin{pmatrix} E \\ E \\ 0 \end{pmatrix} \tag{37}$$

From these equations, the following parameters can be derived:

- Current at the transmitter

$$I_{\underline{1}} = \frac{\left(E - jL_0I_0\omega - r_0I_0\right)\left(jL_2w\omega + r_2 + R_C + \dfrac{1}{jC_2\omega}\right)}{\left(jL_1\omega + r_1\right)\left(jL_2w\omega + r_2 + R_C + \dfrac{1}{jC_2\omega}\right) + \left(M\omega\right)^2} \tag{38}$$

- Current at the receiver

$$I_{\underline{2}} = \frac{jM\omega\left[\left(-E + jL_0I_0\omega + r_0I_0\right)\left(jL_2\omega + r_2 + R_C + \dfrac{1}{jC_2\omega}\right)\right]}{\left(jL_2\omega + r_2 + \dfrac{1}{jC_2\omega} + R_C\right)\left[\left(jL_1\omega + r_1\right)\left(jL_2\omega + r_2 + \dfrac{1}{jC_2\omega} + R_C\right) + \left(M\omega\right)^2\right]} \tag{39}$$

- The power supplied by the transmitter

$$P_1 = \frac{1}{2} Re\left(E \cdot \underline{I_1}\right) = \frac{1}{2} Re\left[\left(\frac{1}{jC_1\omega} + jL_0\omega + r_0\right) I_0 + \left(\frac{-1}{jC_1\omega}\right) I_1\right] \underline{I_1} \quad (40)$$

- The average power transmitted to the load resistance

$$P_2 = \frac{1}{2} R_C \left|\underline{I_2}\right|^2 \quad (41)$$

2.3.6. Selection of $L_0, L_1, L_2, C_1, C_2, r_1, r_2$ Coil and Capacitor Parameters

Inductances L_0, L_1, L_2 of coils

Since the coils are coreless, the inductance is derived by

$$L = \frac{\mu_0 N^2 S}{l} \quad (42)$$

The coils used are identical, thus, $L_0 = L_1 = L_2$

- L : Henry inductance (H)
- μ_0 : the magnetic constant ($4\pi \cdot 10^{-7}$ H·m^{-1})
- N : the number of windings (155,000)
- S : Cable section (1.5 mm^2)
- l : coil length (45 m)

- **The internal resistances of the coils r_1 and r_2**

$$R = \frac{\rho \cdot L}{S} = \frac{4 \cdot \rho \cdot L}{\pi \cdot D^2} \quad (43)$$

The primary and secondary coils being identical, we have $r_1 = r_2$

- ρ : resistivity of copper (17×10^{-9} Ω·m)
- L : Length of copper wire (45 m)
- S : Cable section (1.5 mm^2)

- **The capacitances of capacitors C_1, C_2**

In order to create coupled resonance phenomenon between the transmitter and the receiver, it is essential that the two capacitors have the same characteristics. Thus, $C_1 = C_2$.

In addition, the capacitor must be selected to give a resonant frequency in the order of kHz.

At resonance, the capacitance of the capacitor is derived by Equation (44).

$$C = \frac{1}{4\pi^2 f^2 L} \quad (44)$$

L : coil inductance

f : resonance frequency

The design values for the wireless transmission circuit components are given in Table 1.

Table 1. Characteristics of the equipment constituting the WETS system.

Equipment	Values
Inductance L_1 of the primary coil	0.001 H

Continued

Inductance L_2 of the secondary coil	0.001 H
Self-inductance L_0	0.001 H
Internal resistance r_1 of the coil from primary	0.5 Ω
Internal resistance r_2 of the coil from secondary	0.5 Ω
Capacitance of the primary capacitor C_1	0.5 μF
Capacitance of the secondary capacitor: C_2	0.5 μF
Load resistance R_C	15 Ω

3. Results and Discussion

The Visual Studio Code software, which is a code editor for the computer development of applications, software, websites, and application services in Javascript, TypeScript, Python, Java, Markdown, C/C++, JSON, PowerShell, HTML/CSS, C#, PHP, or YAML, is used to model the wireless power transfer with inductive coupling. Different simulations were performed for the five configurations presented above, namely: 1) non-resonant circuit, 2) circuit with resonant in the primary, 3) circuit with resonant in the secondary, 4) circuit with resonant in the primary and in the secondary, and 5) circuit with resonance enhancement.

The simulations were performed in the worst case possible, *i.e.* when the coupling coefficient between the two coils is as low as possible ($K = 0.1$). The low value of this coefficient also reflects the fact that the transmitter and receiver coils are as far apart as possible. When the coils are very close to each other, *i.e.* $K = 1$, the system characteristics (efficiency and power) are optimal, which reduces the transmission distance, because the receiver must be very close to the transmitter in all circumstances. Since the aim of this work is to optimize the transmitted power and the system efficiency when the transmitter and receiver are far apart, the value of the coupling between the transmitter and receiver coils is taken to be $K = 0.1$. This value reflects the fact that the two inductances are very far apart. The characteristic curves of the current, powers and efficiency are plotted as a function of E. The value $E = 100$ V was chosen. It allows having the maximum values of the current, powers and efficiency. We chose this value E because, given that the efficiency and power at the emitter and receiver are proportional to E, it is important to choose a high value for E to obtain good output values and also to ensure that this value is more or less realistic in both simulation and practice.

As for the resonant frequency, it is determined by the inductance and capacitance values. Since the inductance and capacitance values are the same at the emitter and secondary windings, the resonant frequency of the primary is identical to that of the secondary. In this case, we speak of coupled resonance.

3.1. Non-Resonant Circuit

The variations as a function of frequency of the current (a), the active powers on

the primary and secondary (b), the phase shift between the current and the voltage (c), and the system efficiency (d) in the case of inductive coupling without resonance are given in Figure 7.

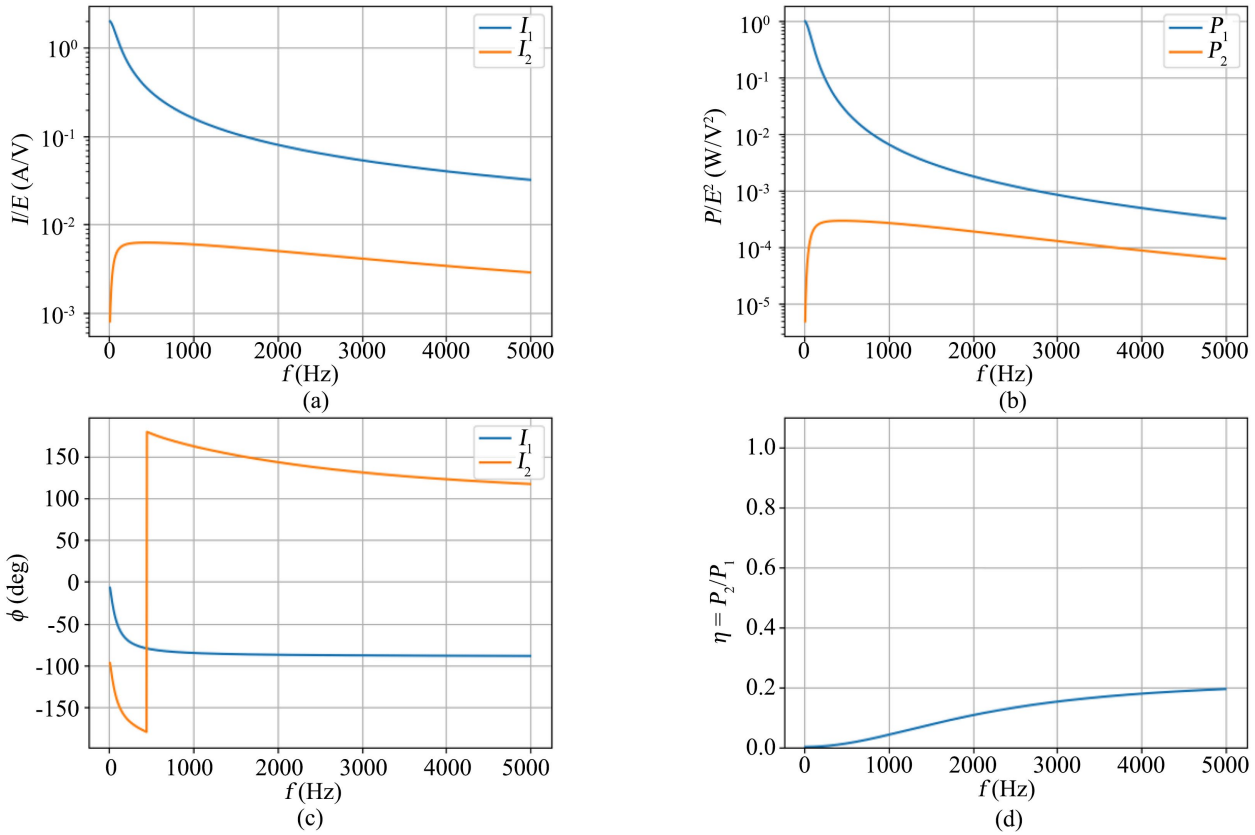

Figure 7. Current (a), powers (b), current-voltage phase shift (c), and efficiency (d) of the electrical circuit of inductive coupling with a real coil, without resonance.

From Figure 7, it is seen that the current in the primary and secondary (Figure 7(a)) decreases as the frequency increases. Also, the powers in the primary and secondary (Figure 7(b)) decreases with the frequency. As the frequency increases, the efficiency increases (Figure 7(d)), until it reaches 20%. At maximum efficiency, the frequency is worth $f = 5$ kHz. The currents and powers in the primary and secondary are respectively: $I_1 = 3.2$ A, $I_1 = 0.28$ A, and $P_1 = 3.2$ W; $P_2 = 0.63$ W. Note that the current in the secondary is very low and the current in the primary is 11.4 times higher than that in the secondary. This means that the power not transferred to the load is dissipated by the Joule effect.

3.2. Circuit with Inductive Coupling and Resonance in the Secondary

The curves in Figure 8 show the variations as a function of the frequency of the current (a), the active powers on the primary and secondary (b), the phase shift between the current and the voltage (c), and the efficiency of the system (d) in the case of an inductive coupling with resonance in the secondary.

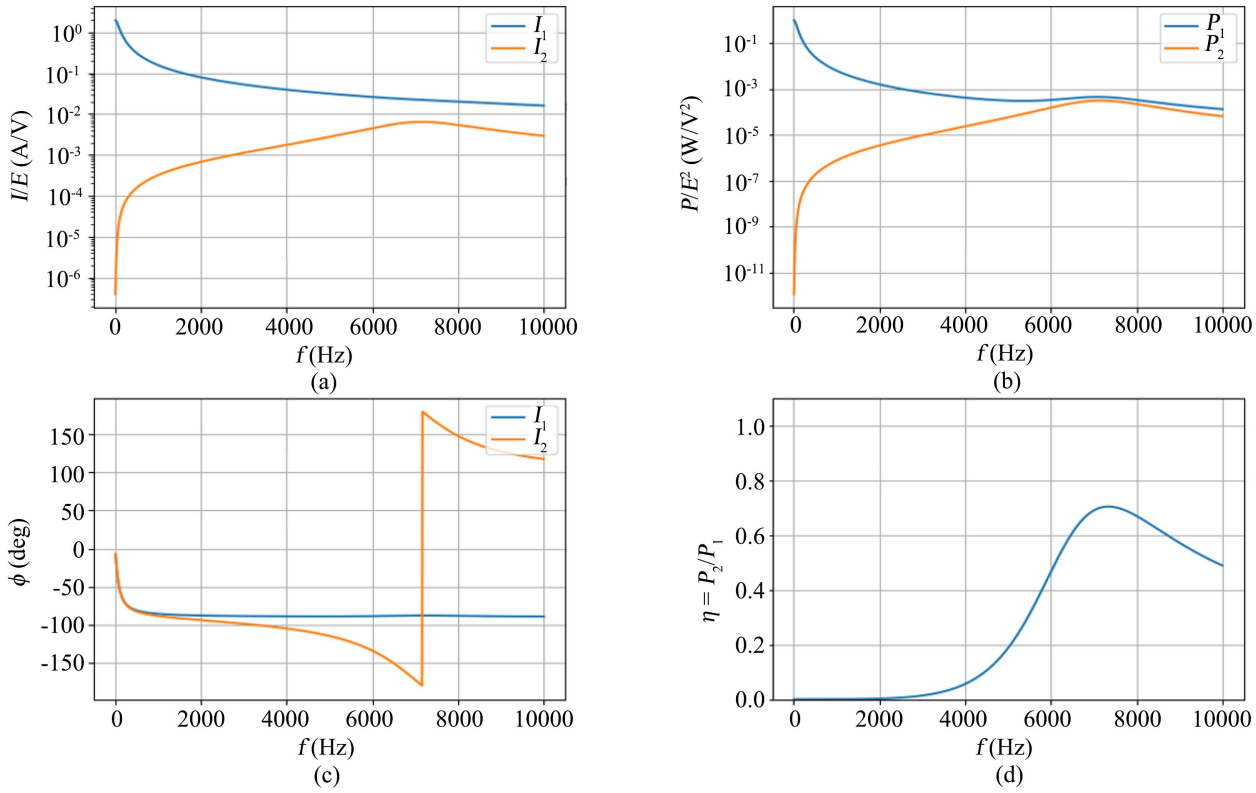

Figure 8. Current (a), powers (b), current-voltage phase shift (c) and efficiency (d) of the electrical circuit with inductive coupling and resonance in the secondary.

It can be seen that when a capacitor is placed in series on the secondary, the power curve on the primary decreases between 0 and 5 kHz, before increasing slightly between 5 kHz and 7.12 kHz, and then decreasing again between 7.12 kHz and 10 kHz. As for the secondary power, it first increases to a maximum 7.12 kHz and then decreases slightly between 7.12 kHz and 10 kHz. The efficiency is initially constant and equal to zero between 0 and 2 kHz. It then started to increase from 2 kHz until it reached its maximum value of 70% $f = 7.12$ kHz. Around this frequency, the efficiency increases significantly. This frequency is the resonant frequency of the secondary circuit. At the resonant frequency, the primary and secondary currents and powers are as follows: $I_1 = 2.2$ A, $I_2 = 0.65$ A, and $P_1 = 4.49$ W; $P_2 = 3.14$ W. When there is resonance in the secondary, the power in the load is 5 times greater than when there is no resonance. Similarly, the efficiency resonance in the secondary is 3.5 times higher than that without resonance.

From these results, it can be concluded that in a wireless power transmission system, resonance in the secondary circuit allows a significant improvement in power efficiency but its effect on the power transmitted to the load is weak. This result is justified, because the phase shift between the current and the voltage (at the source terminals) in the primary circuit remains very close to $-\pi/2$. Thus, the impedance seen from the source remains quasi-inductive despite the resonance in the secondary circuit.

3.3. Circuit with Inductive Coupling and Resonance in the Primary

Figure 9 shows the variations as a function of frequency of the current (a), the active powers at the primary and secondary (b), the phase shift between the current and the voltage (c), and the system efficiency (d) in the case of an inductive coupling with resonance in the primary. It can be seen that when a capacitor is placed on the primary, the primary and secondary currents increases until they reach the values $I_1 = 154$ A and $I_2 = 15$ A respectively, at the resonance frequency of 7.12 kHz. From this frequency, the two curves decrease until they reach the values $I_1 = 8.5$ A and $I_2 = 0.81$ A. The power of the primary increases until it reaches the maximum value $P_1 = 7.72$ kW at the resonance frequency of 7.12 kHz, and then decreases until it reaches the value $P_1 = 140$ W. The power of the secondary follows the same curve as the primary, with the difference that at the resonance frequency, $P_2 = 1.7$ kW. The efficiency increases from 0 to 10 kHz, until it reaches its maximum value of 22%. Thus, when there is resonance in the primary of a wireless power transmission system, the power delivered to the load is approximately 541 times higher than the power in the load for a circuit with resonance in the secondary, and 2698 times higher than the power for a circuit without resonance**.** On the other hand, the efficiency of the system with resonance in the primary is 3 times lower than the efficiency of the circuit with resonance in the secondary.

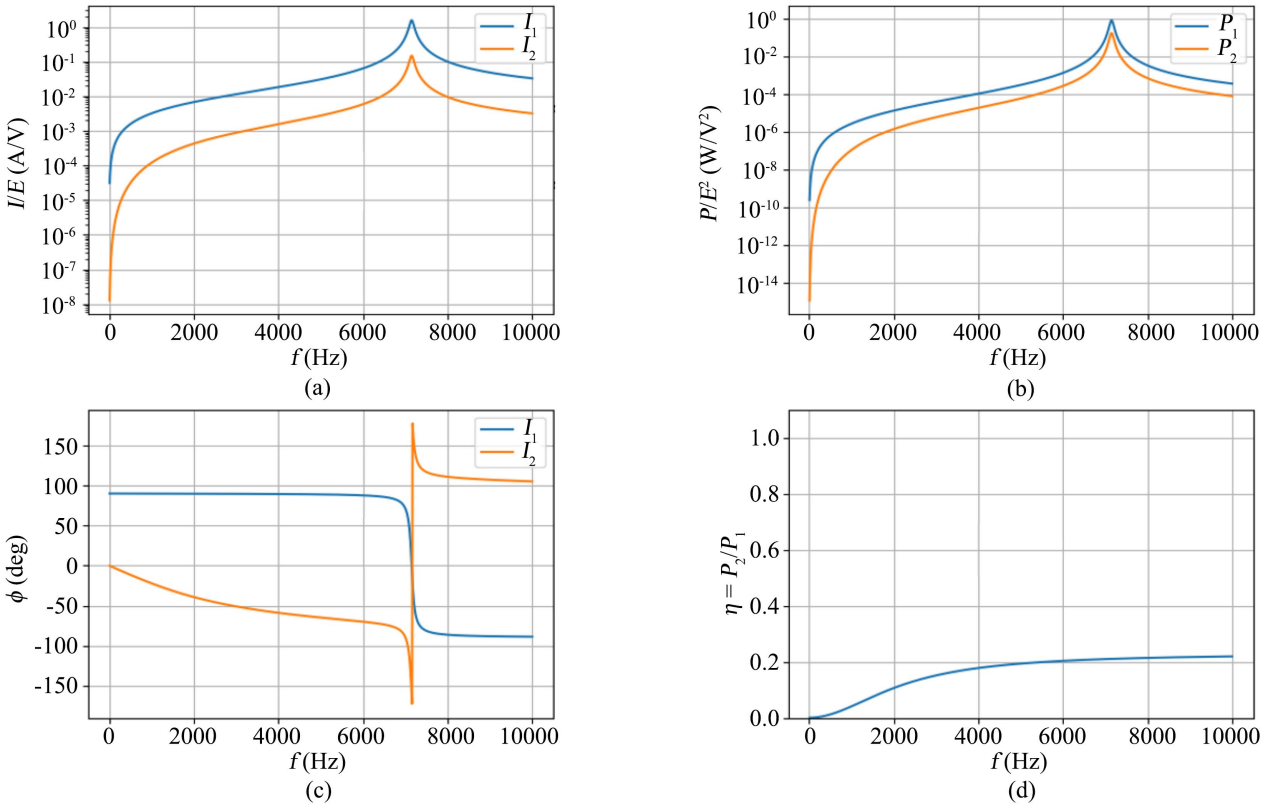

Figure 9. Current (a), powers (b), current-voltage phase shift (c) and efficiency (d) of the electrical circuit with inductive coupling and resonance in the primary.

These results show that the resonance in the primary does not provide any gain in efficiency, but it does allow for significant values of the power transmitted to the load and the current in the load. In fact, the phase shift between the current and the voltage (at the source terminals) in the primary circuit is zero at resonance, which maximizes the power transmitted at this frequency.

3.4. Circuit with Inductive Coupling and Resonance in the Primary and in the Secondary

The variations as a function of frequency of the current (a), the active powers at the primary and secondary (b), the phase shift between the current and the voltage (c), and the system efficiency (d) in the case of an inductive coupling with resonance in the primary and in the secondary are given in Figure 10. When capacitors are placed on the primary and secondary, it is observed that the primary and secondary currents increase until they reach the maximum values $I_1 = 55.8$ A and $I_2 = 16.02$ A respectively, at the resonance frequency of 7.12 kHz. The powers at the primary and the secondary increase until they reach the maximum values of $P_1 = 2.28$ kW and $P_2 = 1.94$ kW respectively.

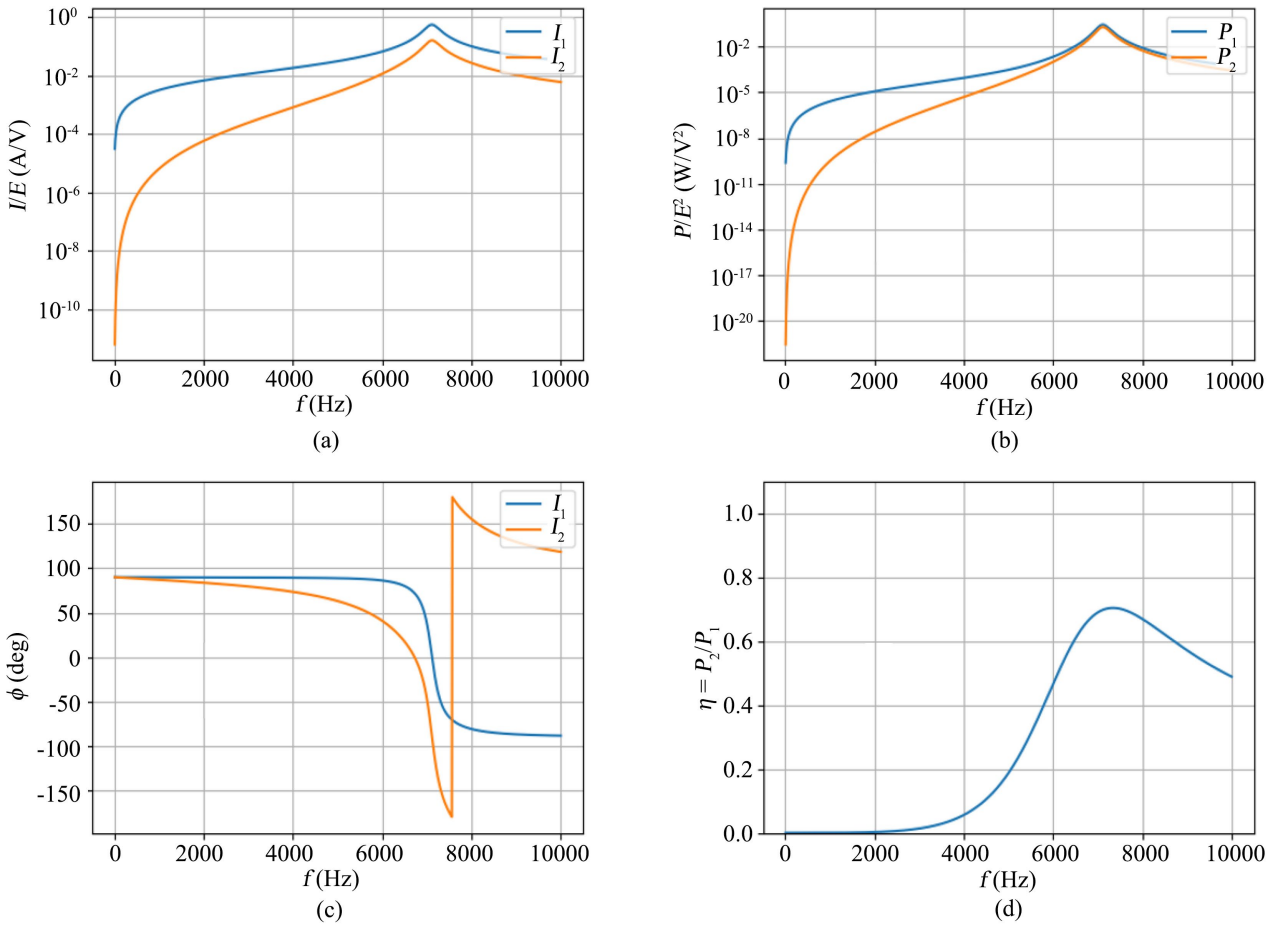

Figure 10. Current intensities (a), powers (b), current-voltage phase shift (c), and efficiency (d) of the electrical circuit with inductive coupling and resonance in the primary and in the secondary.

The efficiency at the resonance frequency is 70%. From these results, it can be concluded that the resonances on the primary and secondary allow a power transfer to the load almost equal to that of a circuit with resonance in the primary. This power is 617 times greater than that of the circuit with resonance in the secondary. The efficiency of the system with resonance in the primary and secondary (coupled resonance) is the same as that of the system with secondary resonance. It is 3 times higher than the efficiency of the circuit with primary resonance. From these observations, it can be conclude that a coupled resonance between the primary and the secondary can increase both the efficiency and the power transmitted to the load.

3.5. Circuit with Improvement of the Resonance

Figure 11 shows the variations as a function of frequency of the current (a), the active powers at the primary and secondary (b), the current - voltage phase shift (c), and the system efficiency (d) in the case of an inductive coupling with resonance improvement. When a capacitor with a self-inductance coil is placed in parallel with the primary, a parallel LC resonance is created. At the frequency of 10.1 kHz, the current in the primary reaches the highest value $I_1 = 92.18$ A compared to all the circuits previously studied. The primary and secondary powers reach their maximum values $P_0 = 4352$ W and $P_2 = 2034$ W at the resonance frequency $f = 10.1$ kHz . The efficiency reaches its maximum value of 70% at the frequency $f = 7.32$ kHz , which is different from the frequency at which the maximum power in the load is obtained.

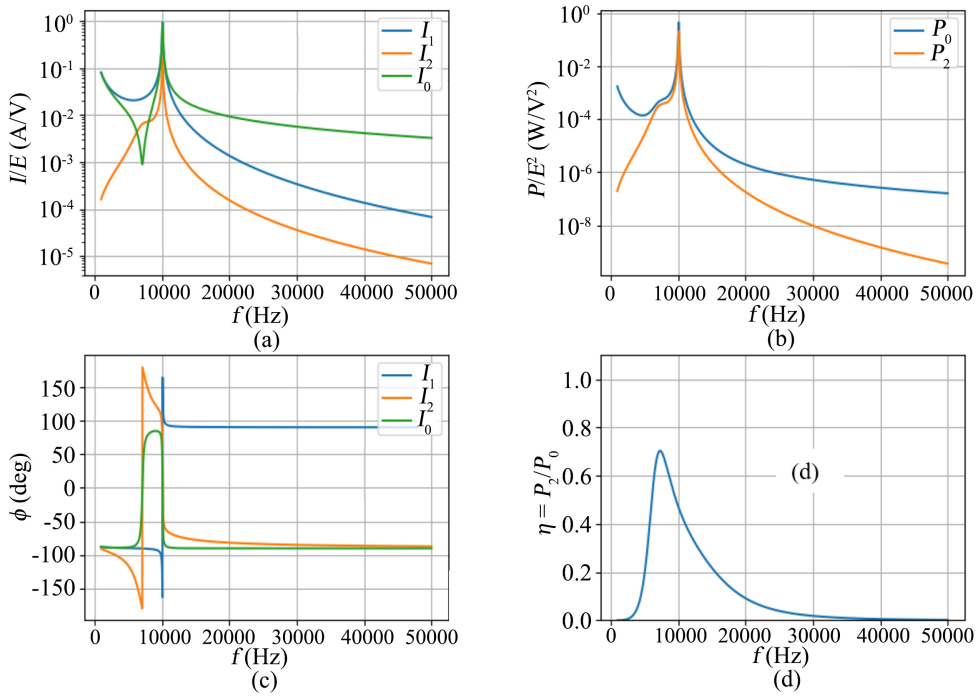

Figure 11. Current (a), powers (b), current-voltage phase shift (c) and efficiency (d) of the electrical circuit with inductive coupling and resonance enhancement.

From the above, it can be concluded that the proposed model with improved resonance allows a power transfer to the load that is approximately 1.04 times higher than that of the circuit with series resonance in the primary and secondary, and approximately 3228 times higher than that of the circuit without resonance. The efficiency is maximum and identical to that of the circuit with series resonance in the primary and secondary, and 3 times higher than that of the circuit without resonance. However, this circuit highlights two notable frequencies, f_1, which maximizes the efficiency ($f_1 = 7.32$ kHz) and f_2 which maximizes the currents and the power transmitted to the load ($f_2 = 10.10$ kHz). This means that the operating frequency is always chosen between the two frequencies in order to maximize either the efficiency or the power in the load. A comparison of the study parameters of the different modelled and simulated circuits is presented in Table 2.

Table 2. Comparison of the secondary current and power, and the efficiency of the circuits studied.

	Circuit without resonance	Circuit with resonance in the secondary	Circuit with resonance in the primary	Circuit with resonance in the secondary and primary	Circuit with improved resonance
Current in the secondary (I_2)	028 A	2.2 A	15 A	16.02 A	16.68 A
Power in the load (P_2)	0.63 W	3.14 W	1700 W	1940 W	2034 W
Yield (η)	20%	70%	22%	70%	70%
frequency	5 kHz	7.12 kHz	7.12 kHz	7.12 kHz	10.1 kHz and 7.32 kHz

From this table, it can be seen that the efficiencies for circuits with the resonance in the primary, the resonance in the primary and secondary and circuit with enhanced resonance have the same maximum efficiency of 70%. Circuits without resonance and with resonance in the primary have lower efficiencies with maximum values of 20% and 22% respectively.

The power transferred to the load with the enhanced resonance circuit is higher than all others in the different cases studied.

It is important to remember that all the results of our study were obtained for a very low coupling coefficient $K = 0.1$. The value of this coefficient indicates that the transmitter and receiver coils are very far apart. If we bring the two coils closer together, *i.e.* approaching k to 0.5 or 0.9, we will obtain very high efficiency and power values in the receiver, *i.e.* 1.5 to 2 times greater compared to those obtained in our study where we considered the most unfavorable case.

3.6. Comparison of the Proposed Configuration with the LCC-S, SP and LCC-LCC Topologies

Table 3 below presents a comparative study between the configuration proposed in this work and the S-P, S-S, LCL-LCL, LCC-S and LCC-LCC topologies, The coupling coefficient is low in each case.

Table 3. Comparison of the proposed configuration with different topologies.

Topology	Output Power (Pout)	Efficiency (η)	Thermal Stability
S-P (Series-Parallel)	0.1 - 0.3 kW	~45% - 55%	Critical (High Heat)
S-S (Series-Series)	0.4 - 0.7 kW	~60% - 68%	Stable
LCL-LCL	1.0 - 1.3 kW	~75% - 79%	Excellent
LCC-S	0.6 - 0.9 kW	~70% - 76%	Stable
LCC-LCC	1.2 - 1.5 kW	~78% - 82%	Excellent
configuration proposed (parallel LC circuit in the primary and series resonance in the secondary)	2034 KW	70%	Excellent

Based on studies [32]-[34], we recorded the maximum power values at the receiver and the efficiency for each of the -P, S-S, LCL-LCL, LCC-S and LCC-LCC topologies.

The table above shows that, with a low coupling coefficient, the proposed configuration allows for a higher power output at the receiver than the maximum values of the S-P, S-S, LCL-LCL, LCC-S, and LCC-LCC topologies. Regarding efficiency, it is higher than the maximum range of the S-P, S-S topology and is approximately in the same range as that of the LCC-S topology, and lower than that of the LCL-LCL and LCC-LCC topology.

3.7. Influence of Variations in the Parameters (L, C and r) of the Transmitter and Receiver

From the previous results, it can be concluded that by creating a parallel resonance associated with a self-inductance coil with a low internal resistance value in the primary on the one hand, and a series resonance in the secondary on the other maximum efficiency and power values in the load can be obtained. For this electrical circuit with inductive coupling and resonance improvement, it is essential to work with the most optimal values of the transmitter and receiver components. This is the aim of this section.

Using the Visual Studio Code software, code was written with the parameters $L_0, L_1, L_2, C_1, C_2, r_1, r_2$, and the simulations were carried out keeping the coupling coefficient K at 0.1. Table 4 gives the ranges and steps of variation of the different parameters.

Table 4. Ranges and steps of transmitter and receiver parameters.

Parameter	Range	Step (300 divisions)
L_0	[0.5 mH; 2.0 mH]	0.167 mH
L_1	[0.5 mH; 2.0 mH]	0.167 mH
L_2	[0.5 mH; 2.0 mH]	0.167 mH
r_1	[0.1 Ω; 1 Ω]	0.1 Ω
r_2	[0.1 Ω; 1 Ω]	0.1 Ω
C_1	[0.1 μF; 1 μF]	0.1 μF
C_2	[0.1 μF; 1 μF]	0.1 μF

The combinations made between different parameters allowed for obtaining nearly 77,960 results, among which were the optimal values of the efficiency and the power transmitted to the load. Thus:

- For the values $L_0 = L_1 = L_2 = 1\,\text{mH}$, $C_1 = 0.5\,\mu\text{F}$; $C_2 = 0.1\,\mu\text{F}$; $r_1 = r_2 = 0.5\,\Omega$ et $f = 22924.92\,\text{Hz}$, the maximum value of the yield is obtained, *i.e.* $\eta = 0.99981$.
- For the values $L_0 = L_1 = L_2 = 1\,\text{mH}$; $C_1 = 0.5\,\mu\text{F}$; $C_2 = 0.5\,\mu\text{F}$; $r_1 = 0.3\,\Omega$; $r_2 = 0.5\,\Omega$ et $f = 10123.12\,\text{Hz}$, the maximum value of the power in the load is obtained, *i.e.* P_2/E^2 =0.702797 for an efficiency of $\eta = 0.88813$. Taking into account the value E = 100 V used during simulations allows to access the value of the power transferred to the load: P_2 = 7027.97 W.

From these observations, it can be concluded that in order to further optimize the system, a careful choice of inductances, capacitances and frequency values must be made and can allow reaching 99.981% theoretical efficiency and 7.02797 kW of theoretical power transferred to the load.

It is important to note that in practice, several losses would need to be considered, which would significantly reduce the theoretically obtained power and efficiency values. These losses include: skin effect, Joule heating losses (conduction), losses in the electronics (inverter and rectifier), and losses in the compensation networks (capacitors and inductors).

4. Conclusions

This work focuses on the study of the optimal transmission of wireless energy. A wireless energy transmission circuit has been studied, taking advantage on the one hand of the effect of resonance in the primary and secondary on the one hand, and on the other hand of a variation of the values of the parameters of the transmitter and receiver, in order to optimize the system in terms of efficiency and power transmitted to the load. Five cases of electrical circuits for wireless energy transmission were studied: a circuit with no resonance, a circuit with series reso-

nance in the primary, a circuit with series resonance in the secondary, a circuit with series - series resonance in the primary and secondary, and a circuit with parallel resonance in the primary and series resonance in the secondary. These electrical circuits were modelled and simulated using Visual Studio Code software. This software was also used to vary the parameters of the transmitter and receiver circuits ($L_0, L_1, L_2, C_1, C_2, r_1, r_2$), in order to optimize the efficiency and the power transferred to the load. The results of the simulations carried out show that the primary resonance allows the power transferred to the load to be to optimized, while the secondary resonance allows the efficiency to be to optimized. The circuit with improved resonance allows for obtaining a maximum of power transferred to the load (about 2034 W at the frequency of 10.1 kHz), and efficiency (70% at the frequency of 7.32 kHz). In the circuit with the proposed resonance improvement, the power transferred to the load is about 1.04 times higher than the power in the circuit with series resonance in the primary and secondary, and 3228 times higher than in the circuit without resonance. The efficiency is maximum compared to the other cases studied; it is 3 times higher than the efficiency of the circuit without resonance. The system was optimized by varying the parameters of the transmitter and the receiver circuits. This allowed a careful choice of inductance, capacitance and frequency values, resulting in a theoretical efficiency of nearly 99.981% and a theoretical power transfer to the load of approximately 7.02797 kW. It should be noted that a study like ours, based solely on simulation, has limitations because it does not take into account various energy losses, component voltage ratings, or magnetic saturation. Therefore, it would be practically difficult to obtain the optimal power and efficiency values we achieved under the same conditions. This is why in the near future, a hardware setup of a wireless transmission circuit using the parameters of the proposed circuit will be built to validate the simulation results obtained in this article, and above all, to evaluate the maximum energy transmission distance.

Availability of Data and Materials

The software used to write the codes below is Visual Studio Code, the download link for which is as follows: Download Visual Studio Code - Mac, Linux, Windows.

- The code used to model and plot the characteristic curves of non-resonant inductive coupling is available at the link: https://drive.google.com/file/d/12R23TfBo9lBD-TdB37V9S29bZu8vYFd6/view?usp=sharing
- The code used to model and plot the characteristic curves of inductive coupling with primary resonance is available at the link: https://drive.google.com/file/d/1wrpD0dkREZ7Z4WKhwodU2pFcyAOqb-sLj/view?usp=sharing
- The code used to model and plot the characteristic curves of inductive coupling with secondary resonance is available at the link: https://drive.google.com/file/d/1tFVHTuwSZ1WnWegP8VTlJWgyfSV-

eDCU/view?usp=sharing

- The code used to model and plot the characteristic curves of inductive coupling with resonance at the primary and secondary is available at the link: https://drive.google.com/file/d/1D-LsATA-GpsKRkEssJcrUYci2iU-kulpW/view?usp=sharing
- The code used to model and plot the characteristic curves of inductive coupling with resonance improvement is available at the link: https://drive.google.com/file/d/16MvD6drzOX-UllNcS04ksdFFxuMbMn8zq/view?usp=sharing
- The code for plotting the powers of the different couplings on the same graph and comparing them is given by the link: https://drive.google.com/file/d/1SP5DdCbPZI1nE-OgGnJ1P8RaFsQMKXKUt/view?usp=sharing
- The code for plotting the yields of the different couplings on the same graph is given by the link: https://drive.google.com/file/d/1N8JTVcPlz8uq7IST8FB8wgal-wfD3LJer/view?usp=sharing

The code used to generate all 77960 results by varying the input parameters (L_0, L_1, L_2, C_1, C_2, r_1, r_2), with the aim of finding the values of the input parameters which maximize the efficiency and the power transmitted to the load, is given by the following link:
https://drive.google.com/file/d/1bEz-WcMv6heqjIkjXtJRLts932_8EZGI9/view?usp=sharing

- The 77,960 results obtained are available from the link: https://docs.google.com/spreadsheets/d/1nRUY3c8fh_UZ_nOqX2FqcK0DXJbE7PBH/edit?usp=sharing&ouid=112509053844273514742&rtpof=true&sd=true

Conflicts of Interest

The authors declare that they have no competing interests.

Authors' Contributions

TKB, NJL and YTA conceived the presented idea. TKB and THE developed the theory, performed the computations, verified the analytical methods and interpreted the results. NJL and YTA interpreted the results and supervised the findings of this work. TKB and THE wrote the manuscript. All authors discussed the results and approved to the final manuscript.

References

[1] Cameroon-Info.Net (2017) Cameroon-Rural Electrification: Only 21.7% of Localities Covered. https://www.cameroon-info.net

[2] Statista Research Department (2024) The Global Smartphone Market—Facts and Figures. Statista.

[3] Vlad, M. (2012) Wireless Energy Transmission. Application to the Remote Awakening of Receivers in Zero-Consumption Standby. Dissertation, University of Lyon.

[4] Greenly. What Is the Ecological Impact of a Battery. https://greenly.earth/fr-fr/blog/actualites-ecologie/empreinte-carbone-batterie

[5] Choi, S.Y., Gu, B.W., Jeong, S.Y. and Rim, C.T. (2015) Fundamentals and Applications of Inductive Power Transfer Systems. *IEEE Journal of Emerging and Selected Topics in Power Electronics*, **3**, 61-74.

[6] Ferrieux, J.P. (2018) Design of a Bidirectional Contactless Energy Transfer System by Induction. Dissertation, University of Grenoble.

[7] Schuder, J.C. (2002) Powering an Artificial Heart: Birth of the Inductively Coupled-radio Frequency System in 1960. *Artificial Organs*, **26**, 909-915. https://doi.org/10.1046/j.1525-1594.2002.07130.x

[8] Schwan, M.A. and Troyk, P.R. (1989) High Efficiency Driver for Transcutaneously Coupled Coils. *IEEE Engineering in Medicine & Biology Society* 11*th Annual International Conference*, Seattle, 9-12 November 1989, 1403-1404.

[9] Vigneau, G. (2016) Study and Modeling of an Energy Transmission System by Inductive Coupling for Electronic Systems in the Automotive Environment. Dissertation, University of Toulouse.

[10] Tesla, N. (1914) Apparatus for Transmitting Electrical Energy. US Patent Number 1,119,732, Issued in Dec. 1914.

[11] Brown, W.C. (1984) The History of Power Transmission by Radio Waves. *IEEE Transactions on Microwave Theory and Techniques*, **32**, 1230-1242. https://doi.org/10.1109/tmtt.1984.1132833

[12] McSpadden, J.O. and Mankins, J.C. (2002) Space Solar Power Programs and Microwave Wireless Power Transmission Technology. *IEEE Microwave Magazine*, **3**, 46-57. https://doi.org/10.1109/mmw.2002.1145675

[13] Kurs, A., Karalis, A., Moffatt, R., Joannopoulos, J.D., Fisher, P. and Soljačić, M. (2007) Wireless Power Transfer via Strongly Coupled Magnetic Resonances. *Science*, **317**, 83-86. https://doi.org/10.1126/science.1143254

[14] Karalis, A., Joannopoulos, J.D. and Soljačić, M. (2008) Efficient Wireless Non-Radiative Mid-Range Energy Transfer. *Annals of Physics*, **323**, 34-48. https://doi.org/10.1016/j.aop.2007.04.017

[15] Ahafhaf, A., EL Abderazak, A., EL Jalouli, M., Materre, D. and Obdam, G. (2014) Wireless Charging of Mobile Phones. Physical Science for Engineering, FIPA17P1G2, SPI.

[16] Wang, W. (2014) Study of Wireless Power Transmission (WPT) Based on Magnetic Coupled Resonance. Dissertation, University of Montréal.

[17] Boudjema, M. (2017) Electromagnetic Study of Wireless Energy Transfer by Series-Parallel Resonant Inductive Coupling. Dissertation, Abderrahmane Mira-Bejaia University.

[18] Zhang, X., Meng, H., Wei, B., Wang, S. and Yang, Q. (2018) An Improved Three-Coil Wireless Power Link to Increase Spacing Distance and Power for Magnetic Resonant Coupling System. *EURASIP Journal on Wireless Communications and Networking*, **2018**, Article No. 131. https://doi.org/10.1186/s13638-018-1148-8

[19] Yan, Y., Shi, W. and Zhang, X. (2020) An Improved Three-Coil Wireless Power Link to Increase Spacing Distance and Power for Magnetic Resonant Coupling System. *EUR-ASIP Journal on Wireless Communications and Networking*, **67**, 1-13.

[20] Taoutaou, K. and Boudechicha, A. (2021) Study and Simulation of a Resonance En-

ergy Transfer System. Dissertation, Mohammed Seddik Ben Yahia Jijel University.

[21] Tag, A. (2022) Pulsed Waveform Optimization for Wireless Power Transfer (WPT). ESYCOM CNRS UMR 9007 Laboratory, Gustave Eiffel University.

[22] Yadav, A. and Bera, T.K. (2023) Ferrite Shielding Thickness and Its Effect on Electromagnetic Parameters in Wireless Power Transfer for Electric Vehicles (EVs). *Journal of Engineering and Applied Science*, **70**, Article No. 132. https://doi.org/10.1186/s44147-023-00298-2

[23] Nebrida, A.P. (2024) Characterization of Resonant Coupled Inductor in a Wireless Power Transfer System. *Journal of Electrical Systems and Information Technology*, **11**, Article No. 8. https://doi.org/10.1186/s43067-024-00134-4

[24] 3GPP (1999) Specific Absorption Rate (SAR) Requirements and Regulations in Different Regions. ARIB TR-T12-34-925 V3.0.0. 113.

[25] IEEE (2006) IEEE Standard for Safety Levels with Respect to Human Exposure to Radio Frequency Electromagnetic Fields, 3 kHz to 300 GHz.

[26] Fernandez, J.M. and Borras, J.A. (2001) Contactless Battery Charger with Wireless Control Link. US Patent Number 6,184,651.

[27] Ka-Lai, L., Hay, J.W. and PGW (2006) Beart, Contactless Power Transfer. US Patent Number 7,042,196.

[28] Moradewicz, A.J. and Kazmierkowski, M.P. (2010) Contactless Energy Transfer System with FPGA-Controlled Resonant Converter. *IEEE Transactions on Industrial Electronics*, **57**, 3181-3190. https://doi.org/10.1109/tie.2010.2051395

[29] Scheible, G., Smailus, B., Klaus, M., Garrels, K. and Heinemann, L. (2003) System for Wirelessly Supplying a Large Number of Actuators of a Machine with Electrical Power. US Patent Number 6,597,076.

[30] Budhia, M., Covic, G.A. and Boys, J.T. (2011) Design and Optimization of Circular Magnetic Structures for Lumped Inductive Power Transfer Systems. *IEEE Transactions on Power Electronics*, **26**, 3096-3108. https://doi.org/10.1109/tpel.2011.2143730

[31] Maouche, B. (2007) Development of Models by Coupled Electromagnetic Quantities: Application to Non-Destructive Control and Evaluation by Eddy Current. Dissertation, Ferhat Abbas-Sétif University.

[32] Li, S.Q., Li, W., Deng, J., Nguyen, T.D. and Mi, C.C. (2015) A Double-Sided LCC Compensation Network and Its Optimization Design for Wireless Power Transfer. *IEEE Transactions on Power Electronics*, **30**, 1-12.

[33] Kan, T., Nguyen, T., White, J.C., Malhan, R.K. and Mi, C.C. (2017) A New Integration Method for an Electric Vehicle Wireless Charging System Using LCC Compensation Topology: Analysis and Design. *IEEE Transactions on Power Electronics*, **32**, 1638-1650. https://doi.org/10.1109/tpel.2016.2552060

[34] Zhang, W., Wong, S., Tse, C.K. and Chen, Q. (2014) Analysis and Comparison of Secondary Series- and Parallel-Compensated Inductive Power Transfer Systems Operating for Optimal Efficiency and Load-Independent Voltage-Transfer Ratio. *IEEE Transactions on Power Electronics*, **29**, 2979-2990. https://doi.org/10.1109/tpel.2013.2273364

List of Abbreviations

AER:	Cameroon Rural Electrification Agency
ICNIRP:	International Commission on Non-Ionizing Radiation Protection
SAR:	Specific Absorption Dose
WETS:	Wireless Energy Transfer System.
S-P:	series-parallel
S-S:	series-series
LCC-S:	inductor-capacitor-capacitor-series
LCL-LCL:	inductor-capacitor-inductor-inductor-capacitor-inductor
LCC-LCC:	inductor-capacitor-capacitor-inductor-capacitor-capacitor